Asian Journal of Physics
Vol. 34, Nos 11-12 (2025) 669-675
Available on: www.asianjournalofphysics.com

ap

Exploring exclusive light dynamics around an exceptional point in an all-lossy dual-core photonic crystal fiber

Shamba Ghosh[1], Arpan Roy[2], Bishnu P Pal[3] and Somnath Ghosh[3]

[1]*Department of Physics, Indian Institute of Technology Jodhpur, Jodhpur-342 030, India*

[2]*Institute of Radio Physics and Electronics, University of Calcutta, Kolkata-700 009, India*

[3]*Department of Physics, École Centrale School of Engineering, Mahindra University, Hyderabad-500 043, Telangana, India*

(In loving memory of Revered Professor M. S. Sodha)

We report the design and analysis of an all-lossy dual-core photonic crystal fiber (PCF) capable of hosting a second-order exceptional point (EP2) without the need for gain. The structure consists of two defect regions acting as cores, embedded within a hexagonal lattice of air holes, with the entire cladding embedded in a fixed background loss. An asymmetric imaginary refractive index distribution between the two cores is used to control modal interaction, enabling coalescence of two modes at the EP2. The existence of the exceptional point is confirmed through the coalescence of both the real and imaginary parts of the complex propagation constants. Furthermore, the branch point topology of the EP2 is validated by tracking the complex modal eigenvalues under a closed parametric loop in the gain–loss parameter space. The proposed all-lossy PCF provides a practical and fabrication-compatible route for realizing non-Hermitian topological singularities, making it a promising platform for next-generation integrated photonic devices based on exceptional point physics.

doi: 10.54955/AJP.34.11-12.2025.669-675

Keywords: Exceptional point, non-Hermitian system, Photonic crystal fiber.

1 Introduction

Non-Hermitian photonic systems have emerged as a versatile platform for exploring novel light–matter interactions, where engineered gain and/or loss enable access to exotic spectral singularities known as exceptional points (EPs). An EP is a non-Hermitian degeneracy where both eigenvalues and eigenvectors of a system simultaneously coalesce, making the overall Hamiltonian defective, which opens up new possibilities of controlling light and device design [1,2]. In particular, second-order EPs (EP2s) — where two modes coalesce — have been shown to exhibit branch-point topology, chiral mode conversion, and enhanced sensitivity to external parameters, making them promising for use in photonic switches, sensors, and topological light transport devices.

Lately, there has been significant progress in the theoretical formulation and experimental demonstration of EP-based photonic systems aimed at enabling unconventional device functionalities [3-6]. These developments hinge on the careful manipulation of non-Hermitian elements—particularly gain and loss—to access and control the topological singularities, i.e., EPs. By tuning such parameters, it becomes possible to engineer branch-point singularities in the system's eigenvalue space and explore the associated nontrivial modal dynamics. EPs of various orders have been explored across a wide range of physical

Corresponding author
e mail: somiit@rediffmail.com (Somnath Ghosh)

platforms, including microcavities [7], optical waveguides [8-10], optomechanical resonators [11], molecular and atomic systems [12,13], and even microwave-scale non-optical structures [14]. These non-Hermitian singularities have drawn increasing interest for their unique ability to enable diverse functionalities such as asymmetric mode switching [15,16], ultra-sensitive detection [17,18], topological energy transfer [19], nonreciprocity enhancement [20,21], and coherent perfect absorption [22]. Of particular interest is the asymmetric modal evolution observed when dynamically encircling an EP in parameter space—an effect central to device concepts such as optical mode converters [9], directional lasers [22], and optical isolators [21].

Toward realizing such capabilities, EPs have been hosted in a range of non-Hermitian systems, including planar waveguides and gain-loss-assisted dual-core optical fibers [23,24]. In a recent study, an EP was demonstrated within a cylindrical waveguide comprising of concentric lossy and non-lossy dielectric layers [25]. Optical fibers, long known for their role in communication technology, have also been revisited in the context of exceptional point. Notably, anti-parity-time (APT)-symmetric single-mode fibers were proposed for EP-induced light transport in systems where the refractive index satisfies $n(-x) = -n^*(x)$ —an alternative to conventional PT symmetry, which requires a gain–loss balance [26,27]. While these approaches use symmetric or asymmetric complex refractive index modulation to host and manipulate EPs, their realization is often constrained by fabrication challenges, instability due to gain, or limited platform scalability.

The demonstrations of EPs in optical platforms have largely focused on structures that require precise gain–loss balancing and complex refractive index modulation in step-index fibers, planar waveguides, or coupled resonator systems. While such platforms have advanced the understanding of EP-induced topological effects—such as asymmetric mode conversion and modal chirality—their integration into real-world photonic systems remains limited due to challenges in gain management, noise, fabrication scalability, and material stability. In particular, gain-loss-assisted optical fibers, although conceptually rich, face practical hurdles in achieving the necessary non-Hermitian index profiles and values within a fiber-compatible geometry. In this context, an all-lossy passive system that hosts an EP emerges as a practically viable and fabrication-friendly solution [28,29]. At the same time, the remarkable design freedom offered by photonic crystal fibers (PCFs)—widely used for dispersion control, nonlinear optics, and sensing—has yet to be fully explored in the context of EP-based mode engineering [30-32]. With their well-established fabrication via stack-and-draw techniques and the ability to incorporate dopants for localized loss control, PCFs provide a structurally versatile and fabrication-friendly platform that is naturally suited for hosting EPs without requiring optical gain.

In this paper, we demonstrate a dual-core PCF structure with a purely lossy refractive index profile designed to host an EP2. The geometry comprises two defect cores embedded within a hexagonal lattice of air holes, surrounded by a lossy cladding in the background. By introducing asymmetric imaginary refractive indices in the two cores while maintaining symmetry in the real part of the refractive indices, we modulate the interaction strength between two coupled modes. The modal evolution is computed using the finite element method, and the existence of the EP2 is confirmed through the coalescence of both real and imaginary parts of the complex propagation constants. To validate the topological signature of the identified EP, we perform a quasistatic parametric encirclement in the non-Hermitian (γ, τ) parameter space and track the associated modal eigenvalues in the complex plane. This approach confirms the branch-point behavior of the EP, providing a gain-free, compact, and integrable photonic platform for topological mode control. The PCF platform offers greater flexibility in both structural and non-Hermitian parameter design. Taken together, these advantages make PCFs a promising and experimentally viable platform for implementing EP-based photonic functionalities in practical, fiber-compatible architectures.

2 Results and discussions

Designing the all-lossy dual-core PCF

The proposed structure is a dual-core photonic crystal fiber especially designed to support non-Hermitian interactions between modes in the absence of any optical gain. The geometry comprises air holes arranged in a hexagonal pattern in the cladding around two centrally placed defect cores, as shown schematically in Fig 1. Each defect core is formed by omitting an air hole from the periodic lattice, and both cores are symmetrically placed along the horizontal axis with a center-to-center separation of 2Λ, where Λ denotes the pitch of the air-hole lattice. The background silica is modeled with a refractive index $n_0 = 1.45$, and the air-hole diameter d is set such that the ratio $d/\Lambda = 0.29$ ensures guidance and high mode confinement.

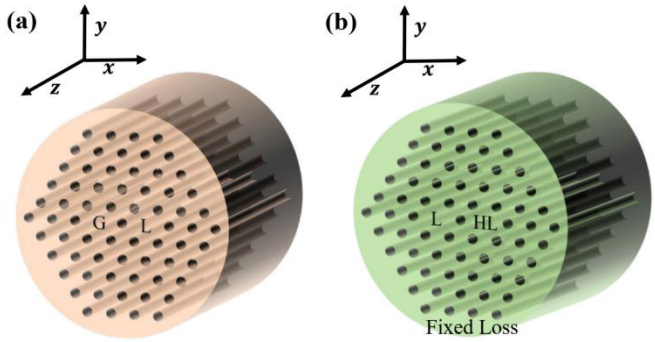

Fig 1. Schematic comparison between (a) the conventional gain-loss-assisted dual-core PCF structure and (b) the proposed all-lossy dual-core PCF design. In the conventional scheme, a symmetric gain–loss profile is introduced in the cores to create non-Hermiticity, typically requiring complex fabrication and stabilization techniques. In contrast, the proposed structure employs a purely lossy configuration, where both defect cores are embedded in a lossy cladding background, and an asymmetric unequal value of the imaginary part of the refractive indices is chosen only for the cores.

To induce non-Hermiticity, we adopt a novel approach in contrast to the conventional method of adding gain to one core and loss to the other fiber core [24]. Instead, we assign a small but uniform loss to the entire cladding. The two defect cores are assumed to be characterized by two loss levels: one having a lower loss, and the other having a higher loss value (indicated in Fig 1(b) as L and HL). In conventional schemes, the cladding is chosen to be passive with gain in one core and loss in the other. Here, we set a fixed low loss value to the cladding and assign each core a distinct loss value—one lower, one higher. This creates an analogous environment to the conventional gain-loss assisted system without introducing any gain into the fiber. Figure 1(b) shows a schematic comparison between the conventional gain-loss approach and the all-lossy configuration we proposed here. The resulting complex refractive index distribution across the structure is defined as follows:

Left core: $n_L = n_c + i(\gamma_{FL} - \gamma)$,

Right core: $n_R = n_c + i\,(\gamma_{FL} + \gamma\tau)$,

Cladding: $n_c + i\gamma_{FL}$

where ($\gamma_{FL} = 5\times10^{-4}$) is the fixed loss, and the loss coefficient γ and the fractional loss ratio τ are the two non-Hermitian parameters that determine the extent of loss contrast between the cores while maintaining a completely gain-free system. Figure 2(a) shows the cross-sectional refractive index distribution of the fiber, with (a.1) depicting the real component of n, and (a.2) displaying its corresponding imaginary component for a specific set of values of $\gamma = 0.00018$, $\tau = 1$. This asymmetric loss distribution modulates the coupling strength and enables the hosting of an EP in the system's parameter space. The real part of the refractive index

remains fixed in both cores to maintain structural symmetry, ensuring that the observed effects stem purely from the non-Hermitian modulation.

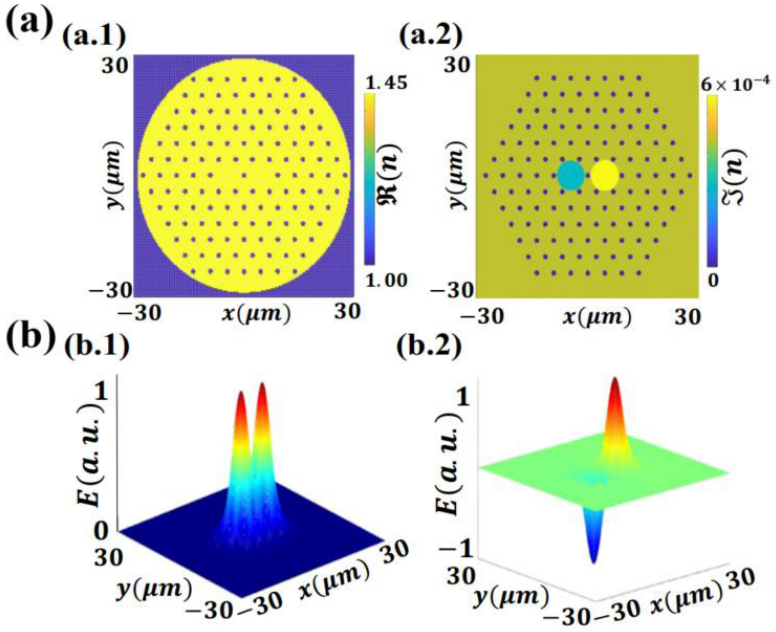

Fig 2. (a) Cross-sectional refractive index profile of the proposed all-lossy dual-core PCF. (a.1) Real part of the refractive index ($Re(n)$), showing two identical defect cores embedded in a hexagonal lattice of air holes. (a.2) Imaginary part of the refractive index ($Im(n)$) for a representative set of non-Hermitian parameters: $\gamma = 0.00018$, $\tau = 1$. A uniform background loss $\gamma_{FL} = 5 \times 10^{-4}$ is applied to the entire cladding, while the two cores are assigned asymmetric loss values, one having a lower loss and the other a higher loss. (b) depicts normalized transverse electric field intensity profiles of the two supported modes, ψ_0 (b.1) and ψ_1 (b.2), respectively.

The mode profiles and the corresponding effective indices are computed using a finite element method (FEM) solver. The numerical mesh is adaptively refined around the defect cores to capture high field gradients, and convergence is verified across multiple mesh densities. Under this configuration, the fiber supports two guided modes— the symmetric fundamental mode (ψ_0) and the antisymmetric higher-order mode (ψ_1) — which exhibit distinct coupling behaviors under varying degrees of loss asymmetry in the cores. The normalized electric field profiles of the two modes have been depicted in Fig 2(b), where (b.1) represents the fundamental mode and (b.2) represents the higher-order mode.

Hosting EP2 in the parameter space

To host an EP2, we systematically study the evolution of the complex propagation constants of the supported modes as a function of the non-Hermitian parameters (γ, τ). These parameters control the relative loss between the two cores, while keeping the real part of the refractive index constant. Vary the loss parameter γ in a range of 0 to 0.0005 for different τ values and examining the variation of the complex effective indices n_{eff} of the two guided modes, denoted as ψ_0 and ψ_1 as a function of γ. Figure 3(a) shows the simultaneous variation of the $R(n_{eff})$ and $I(n_{eff})$ with γ for both the modes, for a fractional loss ratio fixed at $\tau = 1$. It is observed that at $\gamma_{EP} = 0.00018$, the real parts of n_{eff} for both modes coalesce, and simultaneously, their imaginary parts bifurcate. This simultaneous coalescence and bifurcation of eigen modes is a signature of the presence of a second-order exceptional point, where not only the eigenvalues but also the corresponding

eigenvectors of the system merge. The degeneracy results from the interplay between the inter-core coupling and the asymmetric modal attenuation induced by differential loss.

To verify the topological nature of the identified EP2, we implement a quasi-static parameter-space encirclement in the (γ, τ) plane. The trajectory is defined parametrically as an elliptical loop:

$$\gamma(\phi) = \gamma_0 \sin(\phi/2),$$
$$\tau(\phi) = \tau_{EP} + r \sin(\phi),$$

where (γ_0, τ_{EP}) = (0.0005,1), and r = 0.5 is the encirclement radius, and ϕ varies from 0 to 2π, as shown in Fig 3(b). This choice ensures that the loop encloses the EP located at γ = 0.00018, τ = 1, and at the same time, the loss remains equal to the cladding at the beginning and the end of the encirclement. At each point along the loop, the effective indices of the two modes are calculated, and their evolution is tracked in the complex n_{eff} plane.

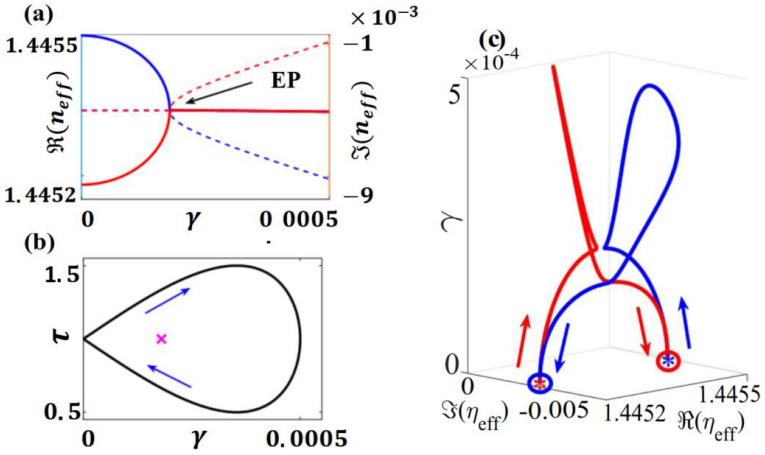

Fig 3. (a) Evolution of the complex effective refractive indices (n_{eff}) of the two guided modes (ψ_0 and ψ_1) as a function of the non-Hermitian loss parameter γ, for a fixed fractional loss ratio τ = 1. The real parts of n_{eff} (solid lines) coalesce, while the imaginary parts (dotted lines) bifurcate at the exceptional point γ_{EP} = 0.00018, confirming second-order non-Hermitian degeneracy. (b) Parametric loop in the (γ, τ) plane used for encircling the EP, defined by Eq (1). The loop is elliptical with γ_0 = 0.0005 (> γ_{EP}) and a fixed radius r = 0.5, ensuring that the EP lies within the encirclement path. (c) Complex-plane trajectories of n_{eff} corresponding to a clockwise (CW) encirclement of the EP along the loop shown in (b). The blue and red curves represent the evolution of the fundamental mode (ψ_0) and higher-order mode (ψ_1), respectively. The trajectories exhibit adiabatic modal exchange characteristic of EP2 behavior. Direction of evolution is indicated by arrows; stars mark the starting points, and circles denote the endpoints of each trajectory.

The resulting trajectories, shown in Fig 3(c), exhibit the signature of adiabatic state exchange: the eigenvalues interchange their positions after a full clockwise traversal, with the starting and ending modes swapping their position on the Riemann surface. This behavior confirms the EP's role as a branch point in the system's parameter space. Importantly, the evolution is smooth and continuous, with no mode crossing or discontinuity, indicating that the system remains in the quasi-static regime and that the EP2 governs the observed modal transformation. This topological mode conversion occurs entirely in a passive, all-lossy environment, without invoking any gain. The ability to realize such modal behavior through controlled loss distribution in a PCF platform highlights a new design route for non-Hermitian photonics. It opens the door to stable, fiber-integrable devices that exploit EP physics for reconfigurable light transport, mode switching, and potentially for enhanced sensing through modal coalescence.

3 Conclusion

In summary, we have proposed and numerically demonstrated a novel all-lossy dual-core PCF platform capable of hosting a second-order exceptional point without requiring optical gain. This configuration not only avoids the instability associated with active gain media but also provides a clean testbed to study purely dissipative non-Hermitian dynamics in guided wave systems. By engineering an asymmetric imaginary refractive index distribution between the two cores, embedded in a lossy background cladding, we achieved modal coalescence in both real and imaginary components of the complex propagation constants. The presence of the EP2 was verified through eigenvalue evolution and further validated via parametric encirclement in the (γ, τ) space, confirming the branch-point topology and adiabatic mode exchange in the complex n_{eff} plane. Unlike prior demonstrations that rely on gain–loss balancing in step-index or slab waveguide structures, our design leverages the structural flexibility and fabrication simplicity of the stack-and-draw method in PCFs. The ability to locally tune optical loss through dopant concentration further enhances experimental feasibility. These features establish the proposed PCF as a practical and integrable platform for realizing non-Hermitian photonic functionalities, offering a robust route toward topological light control, reconfigurable mode conversion, and the realization of future EP-based sensing devices in fiber-compatible systems. Future work may explore higher-order EPs, nonlinear effects, or time-dependent encirclement protocols in this framework, thereby further expanding the scope of PCF-based non-Hermitian photonics.

Acknowledgement

Shamba Ghosh acknowledges the financial support from the Ministry of Education, Government of India.

References

1. Moiseyev N, Non-Hermitian quantum mechanics (Cambridge University Press), 2011.
2. Heiss W, Sannino A, Avoided level crossing and exceptional points, *J Phys A: Math Gen*, 23(1990)1167; doi.10.1088/0305-4470/23/7/022.
3. Eleuch H, Rotter I, Open quantum systems and dicke superradiance, *Eur Phys J: D*, 68(2014)74; doi.org/10.1140/epjd/e2014-40780-8.
4. Eleuch H, Rotter I, Nearby states in non-hermitian quantum systems I: Two states, *Eur Phys J: D*, 69(2015)229; doi.org/10.1140/epjd/e2015-60389-7.
5. Miri M.-A, Alù A, Exceptional points in optics and photonics, *Science*, 363(2019)aar7709; doi. 10.1126/science.aar7709.
6. Bergholtz E J, Budich J C, Kunst K F, Exceptional topology of non-hermitian systems, *Rev Mod Phys*, 93(2021)015005; doi.org/10.1103/RevModPhys.93.015005.
7. Kullig J, Yi C.-H, Hentschel M, Wiersig J, Exceptional points of third order in a layered optical microdisk cavity, *New J Phys*, 20(2018)083016; doi.10.1088/1367-2630/aad594.
8. Doppler J, Mailybaev A A, Böhm J, Kuhl U, Girschik A, Libisch F, Milburn T J, Rabl P, Moiseyev N, Rotter S, Dynamically encircling an exceptional point for asymmetric mode switching, *Nature*, 537(2016)76–79.
9. Zhang X.-L, Wang S, Hou B, Chan C T, Dynamically encircling exceptional points: In situ control of encircling loops and the role of the starting point, *Phys Rev X*, 8(2018)021066; doi.org/10.1103/PhysRevX.8.021066.
10. Ghosh S N, Chong Y D, Exceptional points and asymmetric mode conversion in quasi-guided dual-mode optical waveguides, *Sci Rep*, 6(2016)19837; doi.org/10.1038/srep19837.
11. Liu Z.-X, You C, Wang B, Dong H, Xiong H, Wu Y, Nanoparticle-mediated chiral light chaos based on non-hermitian mode coupling, *Nanoscale*, 12(2020)2118–2125.
12. Lefebvre R, Atabek O, Sindelka M, Moiseyev N, Resonance coalescence in molecular photodissociation, *Phys Rev Lett*, 103(2009)123003; doi.org/10.1103/PhysRevLett.103.123003.

13. Menke H, Klett M, Cartarius H, Main J, Wunner G, State flip at exceptional points in atomic spectra, *Phys* RevA, 93(2016)013401; doi.org/10.1103/PhysRevA.93.013401.
14. Dembowski C, Dietz B, Graf H.-D, Harney H, Heine A, Heiss W, Richter A, Encircling an exceptional point, *Phys Rev E*, 69(2004)056216; doi.org/10.1103/PhysRevE.69.056216.
15. Gilary I, Mailybaev A A, Moiseyev N, Time-asymmetric quantum-state-exchange mechanism, *Phys Rev A*, 88 (2013)010102; doi.org/10.1103/PhysRevA.88.010102.
16. Dey S, Laha A, Ghosh S, Nonlinearity-induced anomalous mode collapse and nonchiral asymmetric mode switching around multiple exceptional points, *Phys Rev B*, 101(2020)125432; doi.org/10.1103/PhysRevB.101.125432.
17. Zeng C, Sun Y, Li G, Li Y, Jiang H, Yang Y, Chen H, Enhanced sensitivity at high-order exceptional points in a passive wireless sensing system, *Opt Express*, 27(2019)27562– 27572.
18. Wong W C, Li J, Exceptional-point sensing with a quantum interferometer, *New J Phys*, 25(2023)033018; doi.10.1088/1367-2630/acc200.
19. Xu H, Mason D, Jiang L, Harris J, Topological energy transfer in an optomechanical system with exceptional points, *Nature*, 537(2016)80–83.
20. Thomas R, Li H, Ellis F M, Kottos T, Giant nonreciprocity near exceptional-point degeneracies, *Phys Rev A*, 94 (2016)043829; doi.org/10.1103/PhysRevA.94.043829.
21. Laha A, Dey S, Gandhi H K, Biswas A, Ghosh S, Exceptional point and toward mode-selective optical isolation, *ACS Photonics*, 7(2020)967–974.
22. Hodaei H, Hassan A, Hayenga W, Miri M, Christodoulides D, Khajavikhan M, Dark-state lasers: Mode management using exceptional points, *Opt Lett*, 41(2016)3049; doi.org/10.1364/OL.41.003049.
23. Bergman A, Duggan R, Sharma K, Tur M, Zadok A, Alù A, Observation of anti-parity-time-symmetry, phase transitions and exceptional points in an optical fibre, *Nat Commun*, 12(2021)486; doi.org/10.1038/s41467-020-20797-7.
24. Roy A, Dey S, Laha A, Biswas A, Ghosh S, Exceptional point-induced asymmetric mode conversion in a dual-core optical fiber segment, *Opt Lett*, 47(2022)2546–2549.
25. Huang Y, Shen Y, Veronis G, Non-PT-symmetric two-layer cylindrical waveguide for exceptional-point-enhanced optical devices, *Opt Express*, 27(2019)37494– 37507.
26. Ge L, Türeci H E, Antisymmetric PT-photonic structures with balanced positive- and negative-index materials, *Phys Rev A*, 88(2013)053810; doi.org/10.1103/PhysRevA.88.053810.
27. Fan H, Chen J, Zhao Z, Wen J, Huang Y.-P, Anti-parity-time symmetry in passive nanophotonics, *ACS Photonics*, 7(2020)3035–3041.
28. Laha A, Biswas A, Ghosh S, Nonadiabatic modal dynamics around exceptional points in an all-lossy dual-mode optical waveguide: Toward chirality-driven asymmetric mode conversion, *Phys Rev Appl*, 10(2018)054008; doi.org/10.1103/PhysRevApplied.10.054008.
29. Roy A, Dey S, Biswas A, Ghosh S, Hosting exceptional point in all-lossy dual-core optical fiber and its exotic chiral light dynamics, *Phys Scr*, 99(2024)055505; doi.10.1088/1402-4896/ad3491.
30. Russell P S J, Photonic-crystal fibers, *J Lightwave Technol*, 24(2006)4729–4749.
31. De M, Gangopadhyay T K, Singh V K, Prospects of photonic crystal fiber as physical sensor: An overview, *Sensors*,19(2019)464; doi.org/10.3390/s19030464.
32. Dudley J M, Taylor J R, Ten years of nonlinear optics in photonic crystal fibre, *Nat Photonics*, 3(2009)85–90.

[*Received*: 19.08.2025; *accepted:* 25.12.2025]